Journal of Catalysis 268 (2009) 175–179

Contents lists available at ScienceDirect

Journal of Catalysis

journal homepage: www.elsevier.com/locate/jcat

Research Note

Identification of the OH groups responsible for kinetic basicity on MgO surfaces by ^{1}H MAS NMR

Céline Chizallet [a,b,1], Hugo Petitjean [a,b], Guylène Costentin [a,b], Hélène Lauron-Pernot [a,b,*], Jocelyne Maquet [c,d], Christian Bonhomme [c,d], Michel Che [a,b,e]

[a] UPMC Univ Paris 06, UMR 7609, Laboratoire Réactivité de Surface, F-75005 Paris, France
[b] CNRS, UMR 7609, Laboratoire Réactivité de Surface, F-75005 Paris, France
[c] UPMC Univ Paris 06, UMR 7574, Laboratoire de Chimie de la Matière Condensée, F-75005 Paris, France
[d] CNRS, UMR 7574, Laboratoire de Chimie de la Matière Condensée, F-75005 Paris, France
[e] Institut Universitaire de France, France

ARTICLE INFO

Article history:
Received 11 May 2009
Revised 27 August 2009
Accepted 6 September 2009
Available online 8 October 2009

Keywords:
^{1}H MAS NMR
MgO
Surface hydroxyl groups
Basicity
Methylbutynol
Catalysis
Spectroscopy

ABSTRACT

Depending on the localization of hydroxyl groups on MgO surface irregularities, their topology and coordination can differ. In order to discriminate their reactivity, three MgO samples with different morphologies are hydroxylated at various levels. From ^{1}H MAS NMR three kinds of OH groups can be distinguished. It is shown that the catalytic activity of base sites in the conversion of 2-methylbut-3-yn-2-ol is governed by species giving a ^{1}H NMR signal at $\delta < -0.7$ ppm, assigned to low coordinated $O_{1C}H$ and $O_{2C}H$ formed by water dissociation on steps and corners. Their reactivity is discussed considering charge and orbital analysis from DFT.

1. Introduction

Examples showing the role of hydroxyl groups (OH) in heterogenous catalytic reactions proceeding on base sites can be found in the literature and are of growing interest because of applications in fine chemistry and biomass valorization. In some cases, improvement of the catalytic results is obtained upon addition of water to the reactant flow like that in aldolic condensation [1], isopropanol decomposition, [2] or oxidative coupling of methane [3]. Oxides such as MgO can also be modified by appropriate pretreatment such as thermal treatment [4], hydration, [5,6] or hydrogenation [7] to exhibit surface OH groups active in isomerization [4], H–D exchange, [6] and alcohol conversion [5,7]. A recent review by Corma and Iborra [8] gives an excellent account of the results obtained on alkaline earth oxides and hydroxides. Moreover, basic OH groups of hydrotalcites have been shown to be catalytically active in aldolic condensation [9,10], Michaël [11] and Claisen–Schmidt [12] condensations, and transesterifications [13].

We investigated earlier the relationship between the thermodynamic Brønsted basicity of a surface, *i.e.*, its ability to displace the deprotonation equilibrium of an acidic molecule and the reactivity of the base sites [5,14]. It was found that, despite a lower Brønsted basicity, hydroxylated surfaces are more reactive in 2-methylbut-3-yn-2-ol (MBOH) conversion, used as model reaction [15], than clean ones.

To first order, two main kinds of hydroxyl groups are expected from hydroxylation of Mg^{2+}_{LC} O^{2-}_{LC} pairs: one resulting from protonation of surface oxide ions O^{2-}_{LC} and one resulting from hydroxylation of the magnesium cation Mg^{2+}_{LC}. They can interact *via* H-bonding but can also be isolated. Moreover, depending on their location on steps, corners, kinks or divacancies, the $O_{LC}H$ groups may exhibit different coordination numbers ($L = 1$, 2, 3, or 4) and thermal stabilities [16].

The aim of this paper is to identify which kind of $O_{LC}H$ group is acting as a base site in MBOH conversion in order to help understanding why, despite a weak Brønsted basicity, they exhibit a high reactivity. In earlier works, it was shown that FTIR could not afford the identification of active sites [17] probably because different kinds of $O_{LC}H$ groups vibrate in the narrow band obtained on hydroxylated MgO surfaces [18] and that their contribution cannot be accurately extracted by spectra decomposition. ^{1}H MAS NMR is

* Corresponding author. Fax: +33 01 44 27 60 33.
E-mail address: helene.pernot@upmc.fr (H. Lauron-Pernot).
[1] Present address: IFP-Lyon, Direction Catalyse et Séparation, BP3, 69390 Solaize France.

0021-9517/$ - see front matter © 2009 Elsevier Inc. All rights reserved.
doi:10.1016/j.jcat.2009.09.003

also an interesting method to characterize OH groups but, in the case of zeolites, the data are in good correlation with IR spectroscopy [19]. Nevertheless some discrepancies to this correlation have already been pointed out in the literature especially in the case of Ca^{2+} and Mg^{2+}-exchanged zeolites [19]. Moreover, as theoretical calculations showed, in the case of MgO, that some species not distinguishable by IR spectroscopy can be differentiated by ^{1}H MAS NMR [20], it was necessary to check whether ^{1}H NMR could afford a distinct evaluation of active sites. Thus, different MgO samples partially hydroxylated were characterized by ^{1}H MAS NMR and by catalysis of the MBOH conversion. In order to rationalize the reactivity of the different OH groups, theoretical calculations of the charge distributions and HOMO/LUMO orbitals energy are performed from a natural population analysis.

2. Experimental

As described earlier [21], MgO samples were prepared by thermal decomposition at 1273 K in vacuum of $Mg(OH)_2$ precursors leading to three materials such as MgO-precipitation, MgO-hydration, and MgO-sol–gel. The BET specific surface areas were found to be 167 $m^2\,g^{-1}$ for MgO-precipitation and 150 $m^2\,g^{-1}$ for both MgO-hydration and MgO-sol–gel. It was checked that there was no surface reconstruction upon hydroxylation treatment [5,21].

The hydroxyl coverage of the samples was controlled by a pretreatment step with identical conditions before ^{1}H MAS NMR and catalysis measurements. The samples are "cleaned up" at 1023 K under nitrogen flow (20 $cm^3\,min^{-1}$). Then, they are cooled down to 373 K and contacted with water vapor flow ($P_{H_2O} = 840$ Pa, flow rate = 20 $cm^3\,min^{-1}$) for 10 min. They are then dehydroxylated at intermediate temperature (473 K < T < 1073 K) in a nitrogen flow (20 $cm^3\,min^{-1}$) for 2 h. In the following, only the final dehydroxylation temperature T that determines the degree of hydroxylation of a sample will be given: MgO-sol–gel-673 is a sol–gel sample that was dehydroxylated at T = 673K.

For NMR experiments, the pretreatment of 125 mg of sample was performed in a "U shape" quartz cell equipped with two valves allowing complete isolation of the system (sample + cell). The pretreated MgO sample system was transferred into a glove box (argon atmosphere; H_2O < 1.5 ppm; O_2 < 3 ppm) where 4 mm (external diameter) zirconia rotors were filled and closed with Kel-F caps. The spectra were recorded at room temperature with a Bruker Avance 400 spectrometer at 9.4 T, equipped with a 4 mm probe and with a spinning rate of 12.5 kHz. A 90° single pulse of 3.3 μs was used with a recycling delay of $5T_1$ over a spectral window of 250 kHz. T_1 was estimated for each sample and each pretreatment temperature, using a Saturation Recovery sequence. The receiver gain remained constant at a value of 200 throughout the experiments, and 128 free induction decays per spectrum were accumulated. The chemical shifts were determined by reference to an external tetramethylsilane (TMS) sample. The signal of the empty rotor was recorded at the same conditions for each experiment. For all spectra, the intensities were normalized to the same specific surface area and the decomposition of the signal was performed with the DMFIT program [22].

The MBOH catalysis reaction was performed as described elsewhere [5]. Wafers were prepared from catalyst powders and crushed into pellets of 125 to 200 μm in diameter. Isosurface area experiments were performed adapting the mass of catalyst loaded in the reactor so as to obtain a surface of 5 m^2 and diluting with SiC (Prolabo, 250 μm diameter) so as to finally reach 75 mg of solid. It was checked that SiC alone does not convert MBOH. After pretreatment, the reactor was cooled to the reaction temperature of 393 K. The MBOH partial pressure (P_{MBOH} = 3.3 kPa) was adjusted by bubbling gaseous nitrogen (100 $cm^3\,min^{-1}$) in liquid MBOH maintained at 303 K. It has been checked by varying the mass of the sample and the inert flow rate that no diffusional limits could be observed under these conditions. Because acetone and acetylene are the only products detected, catalytic data are expressed in terms of conversion only.

Embedded cluster geometry optimizations were performed at the DFT level, within the B3LYP [23,24] hybrid exchange correlation functional, using the Gaussian03 code [25]. Hydroxylated clusters modeling the various surface $O_{LC}H$ groups were previously investigated to obtain their vibrational [18], nuclear [19], and electronic [26,27] properties. The 6-311+G** basis set was used except for third order neighbors (Mg) of hydroxyl groups for which Mg LANL2 effective core potential was used to avoid unphysical polarization with the embedding species (from 913 to 2100 point charges, see Ref. [18]). Charge distributions and HOMO/LUMO orbital occupations were evaluated by a natural population analysis.

3. Results and discussion

In order to perform a quantitative analysis of NMR spectra, in a preliminary work (not reported here), a Hahn-echo procedure was compared to the single pulse procedure. It was concluded that the Hahn-echo procedure helps to localize the probe and the empty rotor signals on the single pulse spectrum but that, to be accurate, it implies a very important number of scans and prohibiting time. Thus, for quantitative analysis, the single pulse procedure was selected, and the broad bands relative to protons of the probe and rotor were modeled by Gaussians on the spectrum acquired with the empty rotor in the same conditions.

2D NOESY NMR experiments [20] showed that at least five maxima can be observed on the spectra thus helping their decomposition as shown in Fig. 1. Assignment of these signals to $O_{LC}H$ groups formed upon water adsorption on MgO defects (see Table 1) was made on the basis of theoretical calculations [20]. It has been shown that three chemical shift domains can be distinguished depending on the nature of the $O_{LC}H$ groups

- $\delta_H > -0.7$ ppm, attributed to most of H-bond donor groups corresponding to signals at 0.8, 0.0, and 0.3 ppm, Fig. 1.
- $\delta_H \approx -0.7$ ppm for the $O_{3C}H$ and $O_{4C}H$ isolated groups (on kinks and divacancies) and for some H-bond donor groups ($O_{4C}H$ on monatomic steps). This contribution is picked up at −0.8 ppm, Fig. 1.

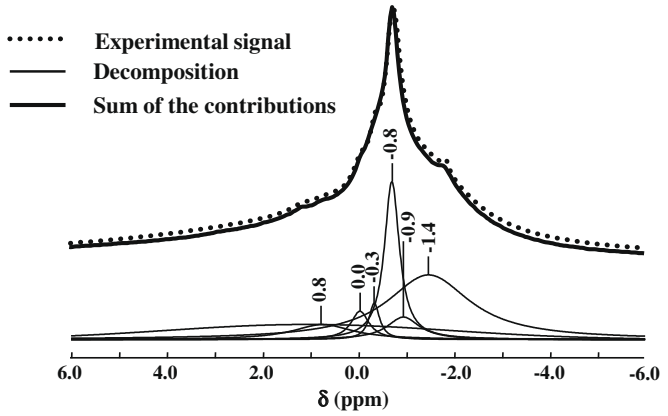

Fig. 1. ^{1}H MAS NMR spectrum (single pulse sequence), corresponding decomposition, and fit of MgO-sol–gel sample after treatment in flowing nitrogen (20 $cm^3\,min^{-1}$) at 1023 K for 1 h, hydration at 373 K (about 840 Pa water diluted in nitrogen (20 $cm^3\,min^{-1}$) for 10 min), and subsequent treatment in flowing nitrogen (20 $cm^3\,min^{-1}$) at 673 K for 2 h.

Table 1
Location, schematic representation, and spectroscopic feature of the different kinds of OH groups modeled earlier [16,18,19].

Location [a]	Molecular description [b]	Location [a]	Molecular description [b]
Monoatomic step	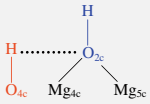	Mg^{2+}_{3C}-terminated corners	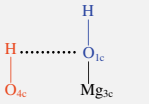
Edge	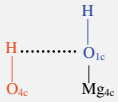	O^{2-}_{3C}-terminated kinks	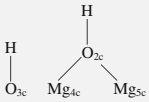
Valley	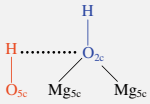	Mg^{2+}_{3C}-terminated kinks	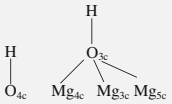
O^{2-}_{3C}-terminated corners	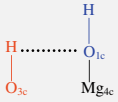	Divacancy	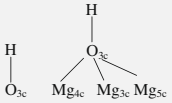

[a] Nomenclature used in former publications.
[b] When H-bonds form, donor OH groups are represented in red and acceptor OH groups in blue. (For interpretation of the references to colour in this table, the reader is referred to the web version of this article.)

– $\delta_H < -0.7$ ppm for $O_{1C}H$ and $O_{2C}H$ groups corresponding to signals at −0.9 and −1.4 ppm, Fig. 1.

The large signals shown in Fig. 1 are due to probe and rotor contributions. The same decomposition was made on the different samples obtained by dehydroxylation at temperatures varying from 673 to 973 K.

The conversion of MBOH was then compared to the integrated area of the NMR contributions at $\delta_H > -0.7$ ppm, $\delta_H \approx -0.7$ ppm, and $\delta_H < -0.7$ ppm. No relationship was found between the MBOH conversion and the amount of OH groups giving a contribution to the two first domains ($\delta > -0.7$ ppm and δ around −0.7 ppm). On the reverse, a good correlation (Fig. 2) is clearly established between the amount of protons giving a signal at $\delta < -0.7$ ppm and MBOH conversion.

From the assignment of this signal to $O_{1C}H$ or $O_{2C}H$ groups a schematic representation of these different kinds of OH groups is given in Scheme 1.

The $O_{LC}H$ ($L = 3$ or 4) counter part can be found in the two domains corresponding to $\delta_H \geqslant -0.7$ ppm explaining why there is

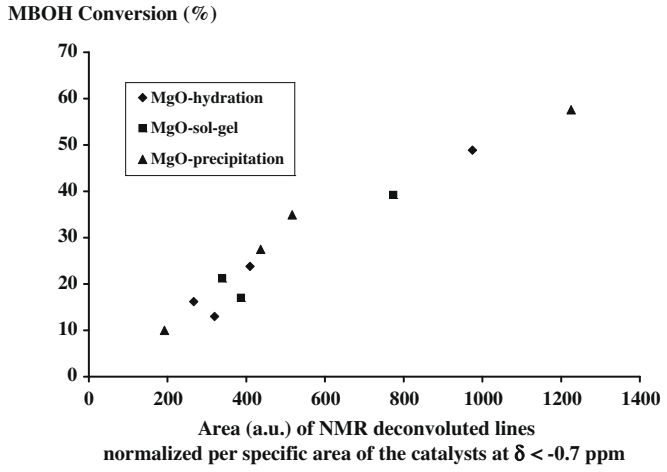

Fig. 2. MBOH conversion in isosurface experiments as a function of the integrated area of the NMR lines corresponding to domain: $\delta < -0.7$ ppm. The experimental points are given for the three MgO samples at different levels of hydroxylation (T varying from 673 to 973 K).

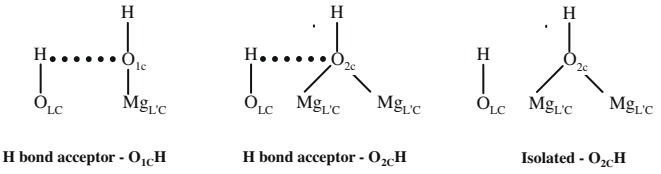

Scheme 1. Molecular description of different catalytically active sites.

no correlation between the catalytic activity and the area of the NMR line located at either $\delta_H > -0.7$ ppm or $\delta_H = -0.7$ ppm independently (data not shown).

The identification of the active sites by ^{1}H NMR allows to understand why these peculiar OH groups cannot be clearly distinguished with FTIR [17] The narrow IR band at 3740 cm^{-1} contains the contributions of H-bond acceptors ($O_{1C}H$ and $O_{2C}H$) identified as active sites by NMR, but also all the isolated $O_{LC}H$. Thus, its area cannot be representative of the amount of active sites.

Now that the active sites have been identified, the mechanism of the reaction on these OH groups can be considered. This is of great interest when considering that if water has often a positive effect in base catalysis by direct addition to the reactants or indirectly by working with a hydroxylated sample, its role played in the mechanism is seldom discussed.

In order to explain the reactivity observed on MgO in a H–D exchange reaction, Hoq et al. [6] proposed a concerted mechanism involving both surface O^{2-} and OH groups: the surface O^{2-} traps the proton (or deuterium) of the alkane molecule while a surface OH group releases a proton. However, in such a cooperative effect between a basic O^{2-} and an acidic OH group (Scheme 2a), a maximum of activity should be expected for partially hydroxylated surfaces, whereas a continuous decrease of MBOH conversion is observed with increasing dehydroxylation temperature and thus for decreasing the OH coverage [5].

So a two-step mechanism in which the first deprotonation step is not necessarily rate-determining (Scheme 2b) can be considered in which the $O_{LC}H$ groups act as Brønsted base sites. In the case of zeolites, the basicity has been often linked to the electrostatic charge on oxygen [28]. Calculation of charge distributions and energies of the HOMO 2p orbitals of O atom are given in Table 2.

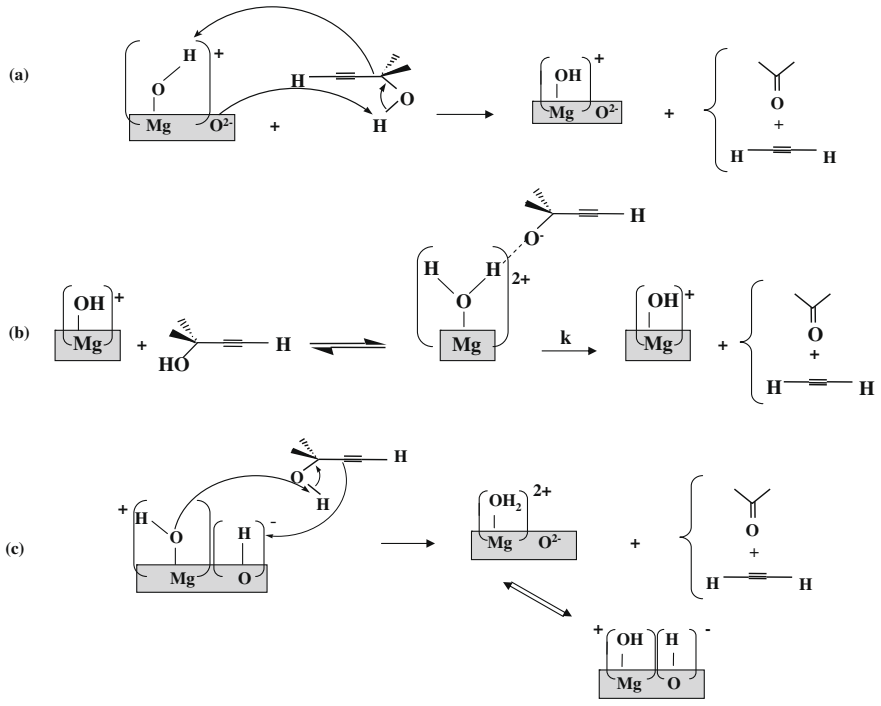

Scheme 2. Different kinds of mechanisms for the conversion of MBOH on OH catalytically active sites.

Table 2
Charge distribution on O and H atoms and energy (Ha[a]) of the 1s orbitals of H atoms and 2p orbitals of O atoms for OH groups on hydroxylated surfaces evaluated by DFT.

System	Mg–O_{LC}–H					$O_{L'C}$–H				
	Type	q_O	$E_{2p}(O)$	q_H	$E_{1s}(H)$	Type	q_O	$E_{2p}(O)$	q_H	$E_{1s}(H)$
Monoatomic step	O_{2C}–H	−1.368	−0.323	0.470	0.148	O_{4C}–H	−1.432	−0.371	0.511	0.126
Edge	O_{1C}–H	−1.352	−0.253	0.472	0.221	O_{4C}–H	−1.470	−0.330	0.520	0.169
Valley	O_{2C}–H	−1.345	−0.274	0.473	0.204	O_{5C}–H	−1.524	−0.356	0.516	0.098
O_{3C}^{2-}-terminated corners	O_{1C}–H	−1.373	−0.207	0.457	0.250	O_{3C}–H	−1.425	−0.258	0.513	0.238
Mg_{3C}^{2+}-terminated corners	O_{1C}–H	−1.384	−0.263	0.473	0.211	O_{4C}–H	−1.447	−0.349	0.522	0.152
Divacancy	O_{3C}–H	−1.386	−0.352	0.481	0.142	O_{3C}–H	−1.434	−0.382	0.489	0.114
Mg_{3C}^{2+}-terminated kinks	O_{3C}–H	−1.389	−0.394	0.481	0.095	O_{4C}–H	−1.399	−0.413	0.485	0.057
O_{3C}^{2-}-terminated kinks	O_{2C}–H	−1.359	−0.086	0.450	0.337	O_{3C}–H	−1.384	−0.173	0.480	0.321

[a] 1 Ha = 27.211 3845(23) eV.

The absolute electrostatic charge on oxygen for a given system is more negative for OH groups formed by protonation of surface oxygen ($O_{LC}H$) than for those formed by hydroxylation of Mg^{2+} ions (Mg–O_{LC}H with L = 1, 2 or 3) (all negative values). According to this criterion, the former should be stronger base sites whereas they are not the active sites. On the other hand, the energy of the 2p orbital of O atom of $O_{LC}H$ groups with L = 1 or 2 which have been identified as active sites is higher than the others. These groups can thus be considered as more reactive toward protonation, and so more nucleophilic. The key parameter governing the reactivity toward MBOH conversion could thus be the nucleophilic character of OH groups.

Another hypothesis has to be considered because as the less-coordinated active $O_{LC}H$ groups (L = 1 or 2) all have a vicinal OH group (Scheme 1), even when they are not H-bonded and called isolated (in the case of O_{3C}^{2-}-terminated kinks). Thus another plausible explanation for the high reactivity of hydroxylated surfaces is the existence of a concerted mechanism (Scheme 2c) involving two vicinal OH groups: one H-donor ($O_{1C}H$ or $O_{2C}H$) and one H-acceptor ($O_{3C}H$ or $O_{4C}H$) even if not involved in H-bonding. This hypothesis is also in agreement with the nature of the active sites identified on the surface because the inactive sites are the OH groups located in divacancies and Mg^{2+}-terminated kinks that exhibit only $O_{LC}H$ vicinal groups with $L \geqslant 3$.

4. Conclusion

The combined use of NMR and catalysis as well as theoretical calculations has led to a refined description of OH groups of MgO catalytically active in the conversion of MBOH. A correlation has been found between the catalytic activity and the amount of OH groups giving a NMR signal at $\delta < -0.7$ ppm. Thus the catalytically active sites could be identified as $O_{1C}H$ and $O_{2C}H$ formed by hydroxylation of the steps, corners, and O_{3C}^{2-}-terminated kinks.

From calculations of the energy of the 2p orbital of O atoms of OH groups, it appears that the active sites have the highest energy, in line with the higher reactivity of these sites and related with what is usually called "nucleophily". Moreover, all the identified active sites have a vicinal OH counterpart that could easily behave as an acid. Thus a concerted mechanism can be considered to explain the high reactivity of these OH groups despite their poor base strength. Work is in progress to evaluate the most plausible mechanism from a theoretical standpoint.

Acknowledgment

The authors acknowledge the financial support of ANR Project: BASICAT, ANR-05-JCJC-0256-01.

References

[1] G. Zhang, H. Hattori, K. Tanabe, Appl. Catal. 36 (1988) 189.
[2] J.A. Wang, X. Bokhimi, O. Novaro, T. Lopez, R. Gomez, J. Mol. Catal. A 145 (1999) 291.
[3] S. Kus, M. Otremba, A. Torz, M. Taniewski, Fuel 81 (2002) 1755.
[4] J.L. Lemberton, G. Perot, M. Guisnet, J. Catal. 89 (1984) 69.
[5] M.L. Bailly, C. Chizallet, G. Costentin, J.M. Krafft, H. Lauron-Pernot, M. Che, J. Catal. 235 (2005) 413.
[6] M.F. Hoq, I. Nieves, K.J. Klabunde, J. Catal. 123 (1990) 349.
[7] T. Yamakawa, M. Takizawa, T. Ohnishi, H. Koyama, S. Shinoda, Catal. Commun. 2 (2001) 191.
[8] A. Corma, S. Iborra, Adv. Catal. 49 (2006) 239.
[9] K.K. Rao, M. Gravelle, J.S. Valente, F. Figueras, J. Catal. 173 (1998) 115.
[10] F. Prinetto, D. Tichit, R. Teissier, B. Coq, Catal. Today 55 (2000) 103.
[11] B.M. Choudary, M. Lakshmi Kantam, C.R. Venkat Reddy, K. Koteswara Rao, F. Figueras, J. Mol. Catal. A 146 (1999) 279.
[12] M.J. Climent, A. Corma, S. Iborra, A. Velty, J. Mol. Catal. A 182–183 (2002) 327.
[13] A. Corma, S.B.A. Hamid, S. Iborra, A. Velty, J. Catal. 234 (2005) 340.
[14] C. Chizallet, M.L. Bailly, G. Costentin, H. Lauron-Pernot, J.M. Krafft, M. Che, Catal. Today 116 (2006) 196.
[15] H. Lauron-Pernot, Catal. Rev. – Sci. Eng. 48 (2006) 315–361.
[16] C. Chizallet, G. Costentin, M. Che, F. Delbecq, P. Sautet, J. Phys. Chem. B 110 (2006) 15878.
[17] C. Chizallet, G. Costentin, H. Lauron-Pernot, J.M. Krafft, P. Bazin, J. Saussey, F. Delbecq, P. Sautet, M. Che, Oil Gas Sci. Technol. 61 (2006) 479.
[18] C. Chizallet, G. Costentin, M. Che, F. Delbecq, P. Sautet, J. Am. Chem. Soc. 129 (2007) 6442.
[19] E. Brunner, H. Karge, Z. Phys. Chem. 176 (1992) 173.
[20] C. Chizallet, G. Costentin, H. Lauron-Pernot, M. Che, C. Bonhomme, J. Maquet, F. Delbecq, P. Sautet, J. Phys. Chem. C 111 (2007) 18279.
[21] M.L. Bailly, G. Costentin, H. Lauron-Pernot, J.M. Krafft, M. Che, J. Phys. Chem. B 109 (2005) 2404.
[22] D. Massiot, F. Fayon, M. Capron, I. King, S. Le Calve, B. Alonso, J.O. Durand, B. Bujoli, Z. Gan, G. Hoatson, Mag. Res. Chem. 40 (2002) 70.
[23] A.D. Becke, J. Chem. Phys. 98 (1993) 5648.
[24] C. Lee, W. Yang, R.G. Parr, Phys. Rev. B 37 (1988) 785.
[25] M.J. Frisch, G.W. Trucks, H.B. Schlegel, G.E. Scuseria, M.A. Robb, J.R. Cheeseman Jr., J.A. Montgomery, T. Vreven, K.N. Kudin, J.C. Burant, J.M. Millam, S.S. Iyengar, J. Tomasi, V. Barone, B. Mennucci, M. Cossi, G. Scalmani, N. Rega, G.A. Petersson, H. Nakatsuji, M. Hada, M. Ehara, K. Toyota, R. Fukuda, J. Hasegawa, M. Ishida, T. Nakajima, Y. Honda, O. Kitao, H. Nakai, M. Klene, X. Li, J.E. Knox, H.P. Hratchian, J.B. Cross, V. Bakken, C. Adamo, J. Jaramillo, R. Gomperts, R.E. Stratmann, O. Yazyev, A.J. Austin, R. Cammi, C. Pomelli, J.W. Ochterski, P.Y. Ayala, K. Morokuma, G.A. Voth, P. Salvador, J.J. Dannenberg, V.G. Zakrzewski, S. Dapprich, A.D. Daniels, M.C. Strain, O. Farkas, D.K. Malick, A.D. Rabuck, K. Raghavachari, J.B. Foresman, J.V. Ortiz, Q. Cui, A.G. Baboul, S. Clifford, J. Cioslowski, B.B. Stefanov, G. Liu, A. Liashenko, P. Piskorz, I. Komaromi, R.L. Martin, D.J. Fox, T. Keith, M.A. Al-Laham, C.Y. Peng, A. Nanayakkara, M. Challacombe, P.M.W. Gill, B. Johnson, W. Chen, M..W. Wong, C. Gonzalez, J.A. Pople, Gaussian 03. Revision C.02, Gaussian Inc., Wallingford CT, 2004.
[26] C. Chizallet, G. Costentin, H. Lauron-Pernot, J.-M. Krafft, M. Che, F. Delbecq, P. Sautet, J. Phys. Chem. C 112 (2008) 16629.
[27] C. Chizallet, G. Costentin, H. Lauron-Pernot, J.-M. Krafft, M. Che, F. Delbecq, P. Sautet, J. Phys. Chem. C 112 (2008) 19710.
[28] D. Barthomeuf, G. Coudurier, J.C. Védrine, Mat. Chem. Phys. 18 (1988) 553.